

Optical bandgap and phase transition in relaxor ferroelectric $\text{Pb}(\text{Mg}_{1/3}\text{Nb}_{2/3})\text{O}_3\text{-xPbTiO}_3$ single crystals: An inherent relationship

X. L. Zhang, Z. G. Hu, G. S. Xu, J. J. Zhu, Y. W. Li, Z. Q. Zhu, and J. H. Chu

Citation: *Applied Physics Letters* **103**, 051902 (2013); doi: 10.1063/1.4816965

View online: <http://dx.doi.org/10.1063/1.4816965>

View Table of Contents: <http://scitation.aip.org/content/aip/journal/apl/103/5?ver=pdfcov>

Published by the [AIP Publishing](#)

Articles you may be interested in

Enhanced dielectric, ferroelectric, and electrostrictive properties of $\text{Pb}(\text{Mg}_{1/3}\text{Nb}_{2/3})\text{O}_3\text{-xPbTiO}_3$ ceramics by ZnO modification

J. Appl. Phys. **113**, 204101 (2013); 10.1063/1.4801881

Electrostrictive effect in $\text{Pb}(\text{Mg}_{1/3}\text{Nb}_{2/3})\text{O}_3\text{-xPbTiO}_3$ crystals

Appl. Phys. Lett. **102**, 152910 (2013); 10.1063/1.4802792

Large and temperature-independent piezoelectric response in $\text{Pb}(\text{Mg}_{1/3}\text{Nb}_{2/3})\text{O}_3\text{-BaTiO}_3\text{-PbTiO}_3$

Appl. Phys. Lett. **101**, 192901 (2012); 10.1063/1.4765347

Structure, piezoelectric, and ferroelectric properties of BaZrO₃ substituted $\text{Bi}(\text{Mg}_{1/2}\text{Ti}_{1/2})\text{O}_3\text{-PbTiO}_3$ perovskite

J. Appl. Phys. **111**, 104118 (2012); 10.1063/1.4722286

Dielectric and piezoelectric activities in $(1\text{x})\text{Pb}(\text{Mg}_{1/3}\text{Nb}_{2/3})\text{O}_3\text{xPbTiO}_3$ single crystals from 5K to 300K

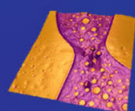
J. Appl. Phys. **111**, 104108 (2012); 10.1063/1.4716031

Asylum Research Atomic Force Microscopes

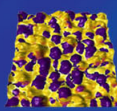
Unmatched Performance, Versatility and Support



The Business of Science®

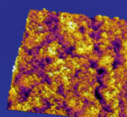


Modulus of Polymers
& Advanced Materials



Piezoelectrics
& Ferroelectrics

Coating Uniformity
& Roughness



Nanoscale Conductivity
& Permittivity Mapping



+1 (805) 696-6466
sales@AsylumResearch.com
www.AsylumResearch.com



Optical bandgap and phase transition in relaxor ferroelectric $\text{Pb}(\text{Mg}_{1/3}\text{Nb}_{2/3})\text{O}_3\text{-}x\text{PbTiO}_3$ single crystals: An inherent relationship

X. L. Zhang (张小龙),¹ Z. G. Hu (胡志高),^{1,a)} G. S. Xu (许桂生),² J. J. Zhu (诸佳俊),¹ Y. W. Li (李亚巍),¹ Z. Q. Zhu (朱自强),¹ and J. H. Chu (褚君浩)¹

¹Key Laboratory of Polar Materials and Devices, Ministry of Education, Department of Electronic Engineering, East China Normal University, Shanghai 200241, China

²R&D Center of Synthetic Crystals, Shanghai Institute of Ceramics, Chinese Academy of Sciences, Shanghai 201800, China

(Received 30 May 2013; accepted 13 July 2013; published online 29 July 2013)

We report band to band transition behaviors of relaxor ferroelectric $\text{Pb}(\text{Mg}_{1/3}\text{Nb}_{2/3})\text{O}_3\text{-}x\text{PbTiO}_3$ (PMN- x PT) single crystals derived from temperature-dependent spectral transmittance. A typical bandgap formula with the temperature and composition ($8\text{ K} \leq T_{\text{exp}} \leq 453\text{ K}$, $0.1 \leq x \leq 0.4$) has been presented. Moreover, the phase diagram of PMN- x PT crystals can be well proposed, which is based on the bandgap variations and can be explained by electronic structure evolution. It reveals an intrinsic relationship between fundamental bandgap and phase transition of PMN- x PT single crystals, which pioneers an effective methodology to explore the phase transition of ferroelectric oxides. © 2013 AIP Publishing LLC. [<http://dx.doi.org/10.1063/1.4816965>]

Single crystals of $\text{Pb}(\text{Mg}_{1/3}\text{Nb}_{2/3})\text{O}_3\text{-PbTiO}_3$ (PMN- x PT) belong to the class of materials known as relaxor ferroelectrics, which have emerged as highly promising multifunctional materials with a strong piezoelectric effect, a high permittivity over a broad temperature range, and unique dielectric response with strong frequency dispersion.¹ It results in a revival of interest in these long-standing fundamental scientific problems. For several decades, these effects have been ascribed to the appearance of polar nanoregions (PNRs), which form spherical or elliptical clusters in a nonpolar matrix at Burns temperature (T_b). The size can be increased due to interactions of the PNR on cooling until the Vogel-Fulcher freezing temperature (T_f).² There is a great interest for these perovskite solid solutions, especially for morphotropic phase boundary (MPB), in which an intermediate phase or coexistence of multiple phases can be found.³⁻⁶ Recently, intense experimental efforts have been made in order to understand phase diagram of PMN- x PT, e.g., synchrotron x-ray powder diffraction,⁷ optical microscopy,⁸ powder neutron diffraction,⁹ and Raman spectroscopy.¹⁰ However, the phase transitions in the MPB region for PMN- x PT system are still contradictory owing to its multi-phase coexistence. Although the above measurements can be accepted for the investigation goal, other useful techniques are indeed desirable with the aid of important properties, such as optical and magnetic response.

As we know, the phase transition is intrinsically related to the crystalline structure variation, which can result in different dielectric response behaviors. Moreover, the electronic bands can be analyzed by assigning the photon-electronic transitions. Therefore, one can expect that there will be a discrepancy among the electronic transitions with different phase structure. Unfortunately, there are few reports on the electronic transitions of PMN- x PT single crystals, especially

in the MPB region. Although the phase transition is a function of temperature and composition, the effects on the electronic band structures have been scarcely reported up to date. From the view of application, the bandgap energy directly determines the maximum working temperature of materials. Moreover, the knowledge of spectral transmittance properties is very desirable, not only for potential practical usage in optoelectronic devices but also to answer basic questions on the energy level of the crystals and physical mechanism of relaxor ferroelectrics. In the MPB region, the interband and/or intraband transitions can become more complex due to the phase coexistence and structure transformation, which result in complicated electronic band structures.

Following the above structural characterizations, we can consider whether it is possible to distinguish the phase structures of PMN- x PT single crystals. At least, there are two distinct advantages: (1) explaining the phase transitions by connecting with the electronic structures; (2) providing the device design parameters with the aid of optical bandgap. Actually, it has been recognized that phase transition can induce variations of bandgap energy.^{11,12} The purpose of this letter is to investigate the relationship between the bandgap and phase transition of PMN- x PT single crystals. Here, a program based on the differences of local regions from the bandgap energy between phases is proposed, which agrees well with the phase diagram proposed previously.⁷ Based on the diagram, we can definitely conclude that the phase transitions can be studied and assigned by temperature-dependent photon-electronic transitions. Through the local features of the observed experimental phenomena and the proposed phase diagram, we connect the characteristics of each region with the corresponding phase, and explore an intrinsic relationship between optical bandgap and phase transition of PMN- x PT single crystals.

The PMN- x PT single crystals are prepared using a vertical Bridgman technique with PT composition of $x = 0.12, 0.24, 0.3, 0.36, 0.37, 0.38,$ and 0.39 , respectively. The samples are cut perpendicular to the $\langle 001 \rangle$ direction.¹³ The

^{a)}Author to whom correspondence should be addressed. Electronic mail: zghu@ee.ecnu.edu.cn. Tel.: +86-21-54345150. Fax: +86-21-54345119.

lattice structure of PMN- x PT crystals is analyzed by X-ray diffraction (XRD) using Cu K α radiation (D/MAX-2550 V, Rigaku Co.). The normal-incident transmittance spectra are recorded by a double beam ultraviolet-infrared spectrometer (PerkinElmer UV/VIS Lambda 950) at the photon energy of 2650-190 nm (0.5–6.5 eV) with the interval of 2 nm. The samples are mounted on a cold stage of an optical cryostat (Janis SHI-4-1) and a heating stage (Bruker A511) for low temperature and high temperature experiments, respectively. The temperature can be varied from 5.3 to 453 K with a resolution of about 0.5 K. Note that no mathematical smoothing has been performed for the experimental transmittance data.

For PMN- x PT single crystals, the spectral loss can be resulted from two factors: the domain walls and the fundamental band absorption. These mechanisms become increasingly important for photon energy near the bandgap. As an example, Figs. 1(a) and 1(b) show the transmittance spectra and XRD data for PMN-12PT crystal, respectively. The absorption edge presents a typical red-shift trend with the temperature, as can be observed from most of semiconductors and dielectrics. In addition, the transmittance in the transparent region decreases at the elevated temperatures. With increasing the temperature, the boundary of the domain region barrier will be a breakthrough easily. The long-range order of the crystal can also be transformed into a short-range order formation. Correspondingly, the ordered domains may be broken into some tiny ordered domains.¹⁴ With the formation of the new domain, more defects are generated inside the crystal. Thus, the introductions of the defect and domain region will cause changes of the transmittance spectra. On the other hand, the XRD patterns show only a single peak in the rhombohedral phase while these are split for the tetragonal structure.¹⁵ No shoulder is found for PMN-0.12PT single crystal, which suggests that it is pure rhombohedral phase at room temperature, as shown in Fig. 1(b). From Fig. 2, however, it can be seen that peaks are split and shift towards a higher diffraction angle with the PT composition. In the MPB region, the XRD peaks split obviously, indicating that it is of tetragonal phase. There also may be monoclinic phase (M) and/or orthorhombic phase (O). Note

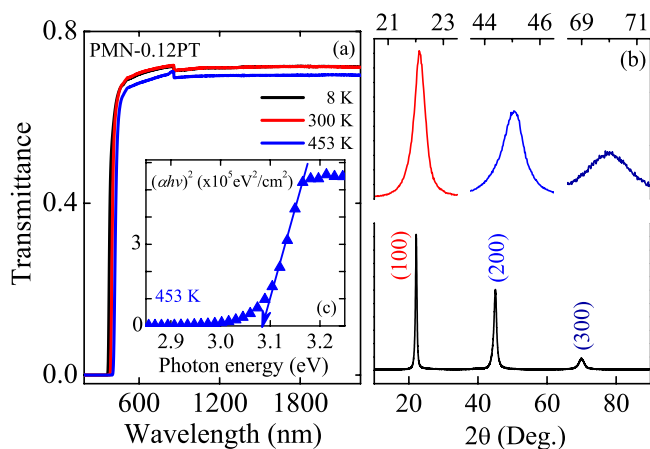


FIG. 1. (a) Temperature dependence of transmittance and (b) XRD patterns for PMN-0.12PT crystal. (c) The function of $(\alpha hv)^2$ as photon energy for PMN-0.12PT single crystal to determine the fundamental bandgap.

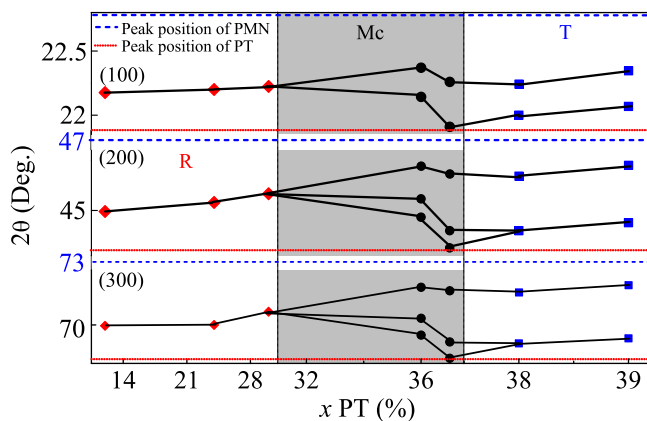


FIG. 2. Composition dependence of diffraction peaks (100), (200), and (300) for PMN- x PT crystals. For comparison, the short dotted and dashed horizontal lines show peak positions of PbTiO_3 and $\text{Pb}(\text{Mg}_{1/3}\text{Nb}_{2/3})\text{O}_3$ crystals, respectively.

that the M phase is a type of monoclinic phase with Pm space group.⁷

Generally, one usually use $(\alpha hv)^2$ (α is absorption coefficient) to determine the bandgap energy, which implies a direct electronic transition.^{16–18} Fig. 1(c) shows the plot of $(\alpha hv)^2$ vs. hv to derive the bandgap. By extrapolating the linear portion of the curve to zero, the bandgap energy can be identified, which are shown in Fig. 3. The phenomenon can be separated into four different regions. Figs. 3(a) and 3(b) are low temperature and high temperature regions of three lower PT compositions, respectively. It can be seen that the bandgap decreases with increasing the temperature except for PMN-0.30PT single crystal. The maximum point that the temperature dependence of the bandgap exhibits for $x=0.3$, which can be due to the different variation trend below and above 300 K. The peculiar characteristic can be ascribed to the monoclinic and rhombohedral multiphase coexistence in the PMN-0.30PT crystal.¹⁹ Figs. 3(c) and 3(d) are low temperature and high temperature regions of four higher PT compositions, respectively. In the low temperature region (below 200 K), the variation rate of bandgap energy for each

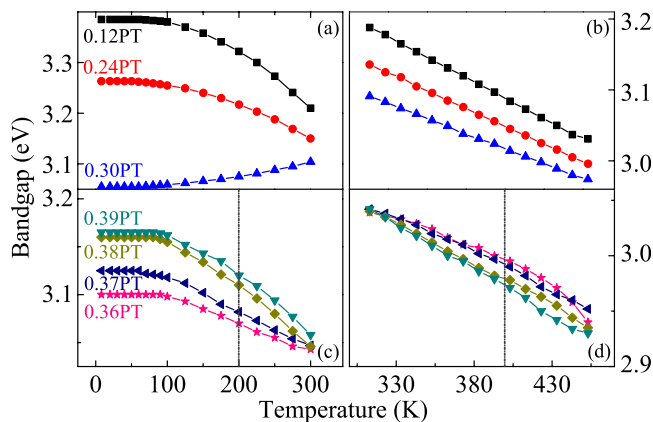


FIG. 3. Bandgap energy of PMN- x PT ($x=0.12, 0.24, 0.30$) at (a) low temperature ($T_{\text{exp}} < 300$ K), (b) high temperature ($T_{\text{exp}} > 300$ K), and bandgap energy of PMN- x PT ($x=0.36, 0.37, 0.38, 0.39$) at (c) low temperature ($T_{\text{exp}} < 300$ K), and (d) high temperature ($T_{\text{exp}} > 300$ K). The bandgap energy decreases as the composition increases in (a), (b), and (d). In contrast, the bandgap energy increases as the composition increases in (c).

composition is kept as the similar value. The curves show a characteristic of quasi-parallel in this region, which can be due to the respective low electronic active and more stable crystal structure. In the high temperature region (beyond 400 K), the cures show a similar characteristic of quasi-parallel. When the temperature approaches Curie temperature (T_c), the ferroelectric-paraelectric phase transition occurs. All crystals belong to a cubic phase (C) structure, which can lead to the stability of the electronic structure. Between 200 K and 400 K, the variation rate of bandgap energy in the MPB region is smaller than these in both of rhombohedral phase (R) and tetragonal phase (T). This may be the main cause of the crossover point as the bandgap of T phase (0.38PT and 0.39PT), which is caught up with a larger decreasing rate than that of Mc phase (0.36PT and 0.37PT). The smaller variation rate of bandgap is due to a multiphase mixing state in the MPB region. It should be emphasized that lattice structure is unstable and the crystal structure is prone to be distorted in the MPB region.

To obtain an empirical formula for the bandgap energy of the relaxor ferroelectric PMN- x PT single crystals on the dependence of temperature and composition, the experiment data are fitted to a standard analytic expression

$$E_g(x, T_{\text{exp}}) = E_0 + E_1(x) + E_2(T_{\text{exp}}) + E'(x, T_{\text{exp}}) + E''(x, T_{\text{exp}}). \quad (1)$$

Here, x represents composition ($0.1 \leq x \leq 0.4$) and T_{exp} represents temperature ($8 \text{ K} \leq T_{\text{exp}} \leq 453 \text{ K}$). E_0 is the bandgap energy of PbTiO_3 , $E_1(x)$ and $E_2(T_{\text{exp}})$ are the main portion of the formula. $E'(x, T_{\text{exp}})$ is the first-order correction to the formula while $E''(x, T_{\text{exp}})$ is the second-order correction. The parameter coefficient with the unit of eV can be obtained as follows:

$$\begin{aligned} E_0 &= 2.515, \\ E_1(x) &= 14.343x - 69.756x^2 + 95.816x^3, \\ E_2(T_{\text{exp}}) &= -1.317 \times 10^{-4}T_{\text{exp}} + 4.245 \times 10^{-6}T_{\text{exp}}^2, \\ E'(x, T_{\text{exp}}) &= (-0.001x + 0.015x^2 - 0.031x^3)T_{\text{exp}}, \\ E''(x, T_{\text{exp}}) &= [(-9.025 \times 10^{-5})x + (4.073 \times 10^{-4})x^2 - (5.41 \times 10^{-4})x^3]T_{\text{exp}}^2. \end{aligned} \quad (2)$$

Note that E_0 fits well with the bandgap energy of PbTiO_3 single crystal with the C phase, which was calculated by local density approximation (LDA) and generalized gradient approximation suggested by Perdew, Burke and Ernzerhof (PBE) model.^{20–23} It is the bandgap energy at the temperature of 766 K, where PbTiO_3 takes a ferroelectric-paraelectric phase transition [4mm (C_{4v}) to $m3m$ (O_h)]. It was reported that the PT composition fluctuation results in polarization variation of PMN- x PT.^{24,25} With increasing PT composition, the birefringent macrodomains will be destroyed, which results in a long-range symmetry breaking.¹⁴ The changes of domain structure imply a variation in the polarization characteristics. When the PT composition falls in the MPB region, the ultrahigh piezoelectric response is attributed to polarization rotation between the T and R

phases through intermediate or monoclinic symmetries. In this region, the proportion of Nb atoms, Mg atoms, and Pb atoms in the crystal lattice reaches a particular value, where the degree of disorder of the lattice becomes maximal. Therefore, some intermediate bandgap may appear which indicates that there is a minimum value in the MPB region.

Temperature is another factor determining polarization characteristics of PMN- x PT crystal. Some experimental results show that the external electric field is applied on the PMN- x PT crystal for polarization inversion^{24,26} and the volume of PNR in PMN- x PT changes with the temperature.^{27–29} When the temperature increases, inherent electric polarization intensity of PMN- x PT crystal can break the balance of shield charge and release the excess shield charge. Bound charges generated by the spontaneous polarization of the crystal are neutralized with the free electrons of the crystal outer surface in the air. The electric moment produced by spontaneous polarization cannot be displayed. The positive and negative charge centers of PMN- x PT crystal take a relative displacement and crystal spontaneous polarization value, which decreases as the temperature increases. It can result in different spectral response behavior.

Fig. 4 shows a three-dimension diagram with two different main perspectives for comparison. All of the fitting lines are well consist with the actual value except for the low-temperature region from the PMN-0.30PT crystal. Moreover, the simulated data match the results reported previously

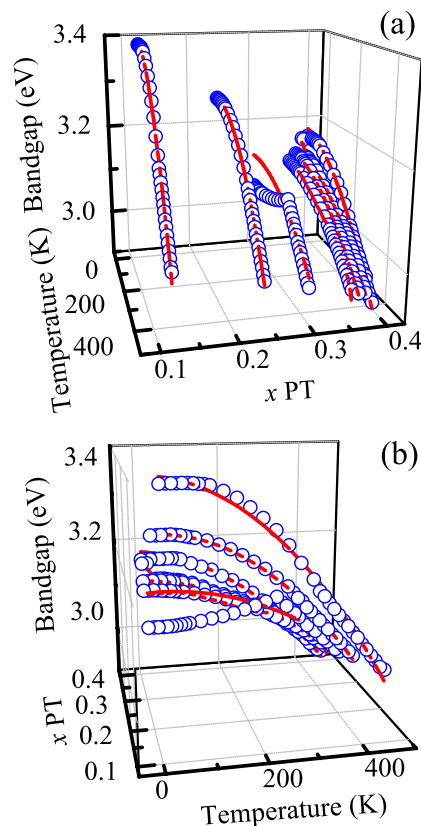


FIG. 4. A three-dimension comparison chart of the fitting and experimental data with main perspective of (a) PT and (b) temperature. The dots and solid lines show the experimental data of the bandgap energy and the fitting values calculated by the formula, respectively.

well, especially for single crystals.¹⁶ In order to present an intuitive distinction of the regional characteristics for the bandgap energies, a three-dimensional map is projected on a plane, as shown in Fig. 5. Surprisingly, it can be found that the picture of the color distribution in the plane is very similar to the bandgap diagram proposed.⁷ For details, Region C is corresponding to the high temperature quasi-parallel region in Fig. 3(b) and the C phase of the phase diagram. Region R is corresponding to the low temperature and low component region in Fig. 3(a) and the R phase of the phase diagram. Region T is corresponding to the interlaced trend region and the T phase of the phase diagram. Region Mc is corresponding to the anomalous temperature phenomenon region of the MPB region at low temperature. This region is corresponding to the quasi-parallel region of the low temperature in Fig. 3(c) and the M phase of the phase diagram.

Fig. 5 presents a phase diagram, which is based on the bandgap derived from temperature-dependent transmittance. Interestingly, it reveals an intrinsic relationship between optical bandgap and phase transition. There are two types of phase transition from the phase diagram. One is a T-C phase transition and a R-C phase transition at high temperature. Another is an R-M-T transition, which occurs at low temperature. In general, the phase diagram presents a negative bandgap narrowing trend with both the temperature and composition. There are two explanations for the negative bandgap narrowing trend with the temperature: thermal expansion of the lattice, and renormalization of the band structure by electron-phonon interaction.³⁰ However, there are two exceptions, where it shows a positive bandgap narrowing trend. A positive bandgap narrowing trend with the temperature appears near the PT composition of about 0.30. Another positive bandgap narrowing trend with the composition appears near PMN-0.39PT crystal. It can be inferred from the present results that the B-O hybridization of PMN is weakly relative to PT as its bandgap energy is larger.³¹ For ABO₃ perovskite structure, chemical disorder leads to strong displacive disorder in the oxygen sublattice driven by B-O hybridization. Consequently, it is commonly believed that the BO₆ octahedron building block determines the basic

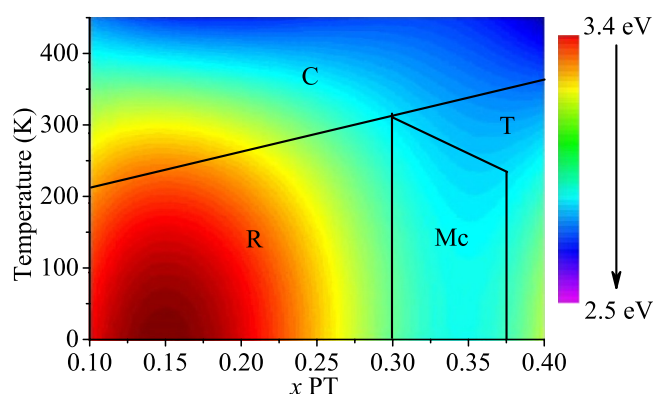


FIG. 5. A phase diagram based on the bandgap energy variation with the temperature and PT composition. The fitting values of Fig. 4 are projected with a color bar, which shows the bandgap variation on temperature and composition. The solid lines distinctly separate the different regions. Note that there are significant differences for the fundamental absorption edge among various phases.

energy level of PMN-*x*PT single crystals. The B-cation *d* orbitals associated with its octahedron govern the lower lying conduction bands (CBs) while the O-anion 2*p* orbitals and its octahedron determine the upper valence bands (VBs). Other ions in the structure contribute to the higher-lying conduction band, which have tiny effects on the fundamental absorption edge.¹⁹ Therefore, the bandgap energy is reduced when the B-O hybridization occurs. In most of the regions, the phase diagram shows a negative bandgap narrowing trend with the composition.

The abnormal temperature dependence of PMN-0.30PT crystal has been recently reported.^{19,32} In this region, the transition phase just appears and there is an coexistence of the R and Mc phases. The Mc phase can be considered as a transitional phase near the MPB region. This area is often referred to a PT-poor region. When the composition *x* is near 0.39, the transition phase has not completely converted to the T phase and there is a mixed state of the T and Mc phases. This area is frequently referred to a PT-rich region. Relatively low thermal stability of PMN-*x*PT crystal has been found in the PT-poor region. This is caused by the stress-relaxation effect, which has been observed for Pb(Zn_{1/3}Nb_{2/3})O₃-*x*PbTiO₃ (PZN-*x*PT) crystals in the PT-poor region near the MPB region.³³ However, the PMN-*x*PT crystal has a relatively good thermal stability in the PT-rich region. It can be seen that the bandgap energy is lower in pure Mc phase region at the same temperature, as compared to other phase region. With increasing PT composition, the influence from the T phase is enhanced. The positive bandgap narrowing trend in the PT-rich region can be attributed to the rapid increment of T domains at the expense of Mc domains, which may lead to the improvement of the total bandgap.

Generally, ferroelectricity is caused by atomic off-center displacements, which results from a delicate balance between long-range Coulomb interaction and short-range covalent interaction.²³ The spontaneous polarization direction and potentials of each phase are closely related to the structural symmetry. Therefore, phase transition of the ferroelectric material is always accompanied by occurrence of the polarization process. When the polarization reaches a threshold, the rotation occurs. For example, external direct-current electric field, pressure, thermal and PT composition will result in changes of domain and dielectric permittivity.³⁴ The transmittance spectra can be used suitably to observe the variations in the structure of PMN-*x*PT internal polarization. As we know, the photons and energy are exchanged with internal particles in the material studied during the light absorbing. When the light frequency reaches the same order of magnitude with the reciprocal of polarization time, the light absorption can approach a high level. Thus, the transmittance spectra show a corresponding response to the internal polarization of PMN-*x*PT induced by the PT composition and temperature. When the polarization process occurs in PMN-*x*PT single crystals, the phase transition process accompanied with a gradient transition or a jumping transition of birefringence corresponds to the fact that optical properties take a gradient transition or a jumping transition, respectively.^{14,35} It is acceptable to investigate phases with the polarization characteristics and the analysis of phases is based on the empirical formula in the present work. The

regional characteristic of bandgap energy is essentially a way to distinguish different phases when the optical properties change after the charge polarization.

To summarize, temperature-dependent spectral transmittance have been investigated for a series of PMN- x PT single crystals ($0.1 \leq x \leq 0.4$). The interesting formula for bandgap energy is presented and expresses the fundamental absorption behavior well. The negative bandgap narrowing trend with the temperature comes from thermal expansion of the lattice and renormalization of the band structure by electron-phonon interaction. However, the positive bandgap narrowing trend comes from the stress-relaxation effect in the PT-poor region and the relative decrement of the M domains. Distinguishing phase is possible through the characteristics of bandgap energy related to the electronic bands. It can be confirmed that spectral transmittance/reflectance is an effective tool to study ferroelectric material.

This work was financially supported by Major State Basic Research Development Program of China (Grant Nos. 2011CB922200 and 2013CB922300), Natural Science Foundation of China (Grant Nos. 11074076, 61106122, and 60906046), Projects of Science and Technology Commission of Shanghai Municipality (Grant Nos. 11520701300 and 13JC1402100), and the Program for Professor of Special Appointment (Eastern Scholar) at Shanghai Institutions of Higher Learning.

¹S.-F. Liu, S.-E. Park, T. R. Shrout, and L. E. Cross, *J. Appl. Phys.* **85**, 2810 (1999).

²H. Takenaka, I. Grinberg, and A. M. Rappe, *Phys. Rev. Lett.* **110**, 147602 (2013).

³M. Ahart, M. Somayazulu, R. E. Cohen, P. Ganesh, P. Dera, H.-k. Mao, R. J. Hemley, Y. Ren, P. Liemann, and Z. G. Wu, *Nature* **451**, 545 (2008).

⁴H. Fu and R. E. Cohen, *Nature* **403**, 281 (2000).

⁵B. Noheda, D. E. Cox, G. Shirane, S.-E. Park, L. E. Cross, and Z. Zhong, *Phys. Rev. Lett.* **86**, 3891 (2001).

⁶S.-E. Park and T. R. Shrout, *J. Appl. Phys.* **82**, 1804 (1997).

⁷B. Noheda, D. E. Cox, and G. Shirane, *Phys. Rev. B* **66**, 054104 (2002).

⁸V. A. Shuvaeva, A. M. Glazer, and D. Zekria, *J. Phys.: Condens. Matter* **17**, 5709 (2005).

⁹A. K. Singh, D. Pandey, and O. Zaharko, *Phys. Rev. B* **74**, 024101 (2006).

¹⁰H. Katzke, M. Dietze, A. Lahmar, M. Es-Souni, N. Neumann, and S.-G. Lee, *Phys. Rev. B* **83**, 174115 (2011).

¹¹V. Sivasubramanian, R. Kesavamoorthy, and V. Subramanian, *Solid State Commun.* **142**, 651 (2007).

¹²R. Farhi, M. E. Marssi, A. Simon, and J. Ravez, *Eur. Phys. J. B* **18**, 605 (2000).

¹³G. S. Xu, K. Chen, D. F. Yang, and J. B. Li, *Appl. Phys. Lett.* **90**, 032901 (2007).

¹⁴Z.-G. Ye and M. Dong, *J. Appl. Phys.* **87**, 2312 (2000).

¹⁵C. He, X. Z. Li, Z. J. Wang, X. F. Long, S. Y. Mao, and Z.-G. Ye, *Chem. Mater.* **22**, 5588 (2010).

¹⁶X. M. Wan, H. L. W. Chan, C. L. Choy, X. Y. Zhao, and H. S. Luo, *J. Appl. Phys.* **96**, 1387 (2004).

¹⁷K. Y. Chan, W. S. Tsang, C. L. Mak, P. M. Hui, and K. H. Wong, *Phys. Rev. B* **69**, 144111 (2004).

¹⁸A. Y. Liu, X. J. Meng, J. Q. Xue, J. L. Sun, J. Chen, and J. H. Chu, *Appl. Phys. Lett.* **87**, 072903 (2005).

¹⁹J. J. Zhu, W. W. Li, G. S. Xu, K. Jiang, Z. G. Hu, M. Zhu, and J. H. Chu, *Appl. Phys. Lett.* **98**, 091913 (2011).

²⁰R. E. Cohen and H. Krakauer, *Phys. Rev. B* **42**, 6416 (1990).

²¹J. P. Perdew, K. Burke, and M. Ernzerhof, *Phys. Rev. Lett.* **77**, 3865 (1996).

²²S. Piskunov, E. Heifets, R. I. Eglitis, and G. Borstel, *Comput. Mater. Sci.* **29**, 165 (2004).

²³R. E. Cohen, *Nature (London)* **358**, 136 (1992).

²⁴R. R. Chien, C.-S. Tu, V. H. Schmidt, and F.-T. Wang, *J. Phys.: Condens. Matter* **18**, 8337 (2006).

²⁵Z. Y. Feng, H. S. Luo, Y. P. Guo, T. H. He, and H. Q. Xu, *Solid State Commun.* **126**, 347 (2003).

²⁶S. J. Zhang, J. Luo, R. Xia, P. W. Rehrig, C. A. Randall, and T. R. Shrout, *Solid State Commun.* **137**, 16 (2006).

²⁷G. Y. Xu, J. S. Wen, C. Stock, and P. M. Gehring, *Nature Mater.* **7**, 562 (2008).

²⁸G. Y. Xu, Z. Zhang, Y. Bing, Z.-G. Ye, and G. Shirane, *Nature Mater.* **5**, 134 (2006).

²⁹I.-K. Jeong, T. W. Darling, J. K. Lee, Th. Proffen, R. H. Heffner, J. S. Park, K. S. Hong, W. Dmowski, and T. Egami, *Phys. Rev. Lett.* **94**, 147602 (2005).

³⁰H. Y. Fan, *Phys. Rev.* **82**, 900 (1951).

³¹D. J. Singh, *Phys. Rev. B* **53**, 176 (1996).

³²J. J. Zhu, W. W. Li, G. S. Xu, K. Jiang, Z. G. Hu, and J. H. Chu, *Acta Mater.* **59**, 6684 (2011).

³³W. S. Chang, L. C. Lim, P. Yang, C.-S. Ku, H.-Y. Lee, and C.-S. Tu, *J. Appl. Phys.* **108**, 044105 (2010).

³⁴C.-S. Tu, I.-C. Shih, V. H. Schmidt, and R. Chien, *Appl. Phys. Lett.* **83**, 1833 (2003).

³⁵F. Cordero, F. Craciun, F. Trequatrini, E. Mercadelli, and C. Galassi, *Phys. Rev. B* **81**, 144124 (2010).